PB90-116146

Dissolution and Crystallization of Calcium Sulfite Platelets

Texas Univ. at Austin

Prepared for:

Environmental Protection Agency, Research Triangle Park, NC

1987

U.S. Department of Commerce
National Technical Information Service
NTIS

AEERL-P-282

TECHNICAL REPORT DATA
(Please read Instructions on the reverse before complet

1. REPORT NO. EPA/600/D-89/187	2.	3. PB90-116146
4. TITLE AND SUBTITLE Dissolution and Crystallization of Calcium Sulfite Platelets		5. REPORT DATE 6. PERFORMING ORGANIZATION CODE
7. AUTHOR(S) Cynthia L. Gleason and Gary T. Rochelle		8. PERFORMING ORGANIZATION REPORT NO.
9. PERFORMING ORGANIZATION NAME AND ADDRESS The University of Texas at Austin Department of Chemical Engineering Austin, Texas 78712		10. PROGRAM ELEMENT NO. 11. CONTRACT/GRANT NO. CR 812454-01
12. SPONSORING AGENCY NAME AND ADDRESS EPA, Office of Research and Development Air and Energy Engineering Research Laboratory Research Triangle Park, NC 27711		13. TYPE OF REPORT AND PERIOD COVERED Published Paper; 9/84-8/86 14. SPONSORING AGENCY CODE EPA/600/13

15. SUPPLEMENTARY NOTES AEERL project officer is Charles B. Sedman, Mail Drop 4, 919/541-7700. Presented at AIChE National Meeting, Houston, TX, 3/29-4/2/87.

16. ABSTRACT The paper discusses the dissolution and crystallization of calcium sulfite platelets. The rates of calcium sulfite dissolution and crystallization are important in slurry scrubbing processes for flue gas desulfurization. The rates affect the scrubber solution composition, SO2 absorption, sulfite oxidation, and limestone utilization. The dissolution and crystallization rates of platelet shaped calcium sulfite crystals were measured in the pH stat apparatus. The solution pH was varied from 3.0 to 6.0. The effects of sulfate content in the solids and solution were also investigated. The measured rates for the platelets were compared to the rates previously determined for agglomerates. It was determined that there are subtle differences between platelet and agglomerated calcium sulfite. The platelet sample with a low solid sulfate content dissolved and crystallized slower than the sample with a high solid sulfate content and the agglomerated samples. The inhibiting effect of dissolved sulfate was also greater for the low solid sulfate sample. The sample with a high solid sulfate content dissolved and crystallized at approximately the same rate as the agglomerates.

17. KEY WORDS AND DOCUMENT ANALYSIS

a. DESCRIPTORS		b. IDENTIFIERS/OPEN ENDED TERMS	c. COSATI Field/Group	
Pollution	Scrubbers	Pollution Control	13B	07A, 13I
Calcium	Slurries	Stationary Sources	07B	11G
Sulfites	Flue Gases	Calcium Sulfites		21B
Platelets	Desulfurization		06P	
Dissolving	Agglomerates		07D	
Crystallization			20B	

18. DISTRIBUTION STATEMENT Release to Public	19. SECURITY CLASS *(This Report)* Unclassified	21. NO. OF PAGES 20
	20. SECURITY CLASS *(This page)* Unclassified	22. PRICE

EPA Form 2220-1 (9-73)

REPRODUCED BY
U.S. DEPARTMENT OF COMMERCE
NATIONAL TECHNICAL INFORMATION SERVICE
SPRINGFIELD, VA. 22161

NOTICE

This document has been reviewed in accordance with U.S. Environmental Protection Agency policy and approved for publication. Mention of trade names or commercial products does not constitute endorsement or recommendation for use.

EPA/600/D-89/187

paper 77b

DISSOLUTION AND CRYSTALLIZATION OF CALCIUM SULFITE PLATELETS

by: Cynthia L. Gleason and Gary T. Rochelle
The University of Texas at Austin
Austin, TX 78712

ABSTRACT

The rates of calcium sulfite dissolution and crystallization are important in slurry scrubbing processes for flue gas desulfurization. The rates affect the scrubber solution composition, SO_2 absorption, sulfite oxidation, and limestone utilization. The dissolution and crystallization rates of platelet shaped calcium sulfite crystals were measured in the pH stat apparatus. The solution pH was varied from 3.0 to 6.0. The effects of sulfate content in the solids and solution were also investigated. The measured rates for the platelets were compared to the rates previously determined for agglomerates. It was determined that there are subtle differences between platelet and agglomerated calcium sulfite. The platelet sample with a low solid sulfate content dissolved and crystallized slower than the sample with a high solid sulfate content and the agglomerated samples. The inhibiting effect of dissolved sulfate was also greater for the low solid sulfate sample. The sample with a high solid sulfate content dissolved and crystallized at approximately the same rate as the agglomerates.

This paper has been reviewed in accordance with the U.S. Environmental Protection Agency's peer and administrative review policies and approved for presentation and publication.

Presented at the AIChE National Meeting, Houston, TX, March 29 - April 2, 1987

Introduction

The dissolution and crystallization of calcium sulfite hemihydrate are important in slurry scrubbing processes for flue gas desulfurization because they affect the scrubber solution composition. Therefore they can affect SO_2 absorption, sulfite oxidation, and lime or limestone dissolution (1). Since stack gases contain oxygen some of the sulfite will be oxidized to sulfate. A mixture of calcium sulfite/sulfate is obtained as the product. The sulfate content of the solids can affect their crystal size and shape. The size and shape of the calcium sulfite crystals determine the ease of dewatering and therefore the economics of waste disposal.

A significant amount of work has been done to characterize and improve the quality of the flue gas scrubber sludge. Ottmers et al. (2) performed experiments to measure the precipitation rate of calcium sulfite. The rate was found to be first order relative to the supersaturation of calcium sulfite. Jones et al. (3) confirmed the formation of a solid solution of calcium sulfite/calcium sulfate hemihydrate. Setoyama and Takahashi (4) determined that the sulfate substitution in calcium sulfite hemihydrate is a function of reaction temperature. Edwards (5) performed crystal sizing studies and determined that crystal size distributions obtained using a Coulter Counter were reliable.

A more recent study by Kelly (6) measured the growth rate of calcium sulfite. He also performed experiments to determine the effects of various chemical additives on the metastable limit and the crystal habit. Alvarez-Dalama (7) performed experiments to determine the nucleation and crystal growth rates of calcium sulfite. Also investigated were the effects of high chloride, magnesium, and sodium levels on the crystal habit.

Tseng and Rochelle (8,9) determined the dissolution and crystallization rates of calcium sulfite in aqueous solutions as a function of pH, dissolved sulfite and sulfate, and temperature. The dissolution rate was accurately modeled by assuming spherical particles in an infinite stagnant solution. The crystallization rate was found to be second order

relative to the calcium sulfite supersaturation. Several different seed crystals were used in these studies. They varied in sulfate content and crystal habit (agglomerates and rosettes).

In this paper the work of Tseng was extended to include the dissolution and crystallization rates of calcium sulfite hemihydrate platelets, since this is the crystal habit most often found in industrial systems. The pH stat method was used to measure these rates. This is the same method that Tseng (10) used. The results are compared to previous work by Tseng (10) in which agglomerated samples of calcium sulfite were used.

Dissolution Theory

Calcium sulfite dissolution can be modeled as mass transfer from spherical particles in an infinite stagnant solution. Tseng (10) discusses in detail the mass transfer theory and the effects of solution composition and particle size on calcium sulfite dissolution. The two adjustable parameters in the model are the solubility product (K_{sp}) and the Sherwood number (Sh).

The K_{sp} (Equation 1) is important because it determines the boundary condition at the particle surface.

$$K_{sp} = [a_{Ca^{++}}][a_{SO3^{=}}] \qquad (1)$$

Solids with different sulfate contents have different K_{sp} values. The Sherwood number is a dimensionless group for mass transfer (Equation 2).

$$Sh = k_c d_p / D \qquad (2)$$

For small spherical particles in a stagnant solution, the value of the Sherwood number is 2.0 (11).

For a single spherical particle the rate of dissolution is given by Equation (3).

$$\frac{dV}{dt} = - \frac{Sh\ \pi d_p (D\Delta C)}{\rho} \qquad (3)$$

where $\Delta C = C - C_S$

Integration of Equation (3) results in the volume fraction remaining of a single particle after time t. For a given particle size distribution, the total fraction remaining is given by the summation over the particle size distribution (Equation 4).

$$F = \frac{V_T}{V_0} = \sum \phi_j \left[1 - \frac{kt}{d_j d_{j+1}} \right]^{1.5} \qquad (4)$$

where $k = 4ShD\Delta C/\rho$

Experimental

Seed Crystal Characterization

Two samples of calcium sulfite hemihydrate were obtained from industrial scrubbers. Sample 1 was prepared from an industrial sample obtained from Acurex Corporation. It was generated during pilot plant testing in which thiosulfate was used as an additive to inhibit oxidation of sulfite to sulfate. Sample 2 was obtained from the hold tank of a scrubber in a power plant. The solids were rinsed with distilled water, filtered, and dried. The solids were characterized (Table 1) by infrared spectroscopy (IR), scanning electron microscopy (SEM), BET surface area measurement, and particle size analysis (Coulter Counter). SEM photographs of the two samples are given in Figures 1 and 2. Table 2 contains the particle size distributions. Both samples were platelet crystals, but sample 1 was low in sulfate content (2.4 mole %) and sample 2 had a high sulfate content (15 mole %). The median particle diameters for the samples were 16 and 14 μm,

respectively. The BET surface area for sample 1 (1.0 m^2/g) was less than that for sample 2 (2.8 m^2/g). Also included in Table 1 are the characteristics of the agglomerated samples previously studied by Tseng (10).

Dissolution Rate Measurement

The dissolution rate of calcium sulfite hemihydrate was determined by the pH stat method. The experimental apparatus was a batch slurry reactor with mechanical stirring and gas sparging. It was the same apparatus that was used in previous studies of calcium sulfite dissolution and crystallization (8-10). The reactor solution contained 0.1 M $CaCl_2$, 10 mM Na_2SO_3, and 2 mM platelet seed crystals. The agitator speed was set at 700 rpm. The reactor was sparged with high purity N_2 before the addition of the calcium sulfite seed crystals. The gas sparger was lifted above the solution level to blanket it with N_2 during the rate measurement. The experiments were performed at room temperature.

As calcium sulfite dissolves, the pH increases. To keep the pH constant, HCl was added to the reactor according to Equation (5).

$$CaSO_3 1/2H_2O + HCl \longrightarrow Ca^{++} + HSO_3^- + 1/2H_2O + Cl^- \qquad (5)$$

The HCl titration rate is not exactly equal to the calcium sulfite dissolution rate. There is an equilibrium relationship which must be included (Equations 6,7).

$$HSO_3^- \overset{K_a}{\rightleftharpoons} SO_3^{=} + H^+ \qquad (6)$$

$$\text{moles } CaSO_{3\ \text{dissolved}} = \text{moles } HCl_{\text{added}} \frac{1 + K_a[H^+]}{K_a[H^+]} \qquad (7)$$

The equilibrium constant K_a used in the rate calculation was determined experimentally by Tseng (10) and has the value 1.1×10^{-6} M^2.

In a dissolution experiment the fraction remaining, F, can be calculated from the volume of HCl titrated as a function of time. With a numerical solution of Equation (4), the value of kt can be calculated as a function of the fraction remaining and the initial particle size distribution, ϕ_j. The time interval for 45 to 55 percent of the solids to dissolve is measured. Then the experimental rate constant can be determined from Equation (8).

$$k = \frac{(kt)_{55} - (kt)_{45}}{t_{55} - t_{45}} \qquad (8)$$

Crystallization Rate Measurement

The crystallization rate of calcium sulfite crystals was also determined by the pH stat method. The agitator speed was set at 450 rpm. The reactor solution (0.1 M $CaCl_2$, 10 mM Na_2SO_3, and 1 mM platelet seed crystals) was sparged and blanketed with N_2 in the same manner as in the dissolution experiments. The experiments were performed at room temperature.

When calcium sulfite crystallizes, $SO_3^=$ is consumed according to Equation (9).

$$Ca^{++} + SO_3^= + 1/2H_2O \text{ —— } CaSO_3\ 1/2H_2O(s) \qquad (9)$$

This causes H^+ to be released into solution to maintain the equilibrium relationship between $SO_3^=$ and HSO_3^- (Equation 6).

This pH drop causes the pH stat to dispense Na_2SO_3 to maintain the pH at the original value. Therefore the crystallization rate of calcium sulfite is equal to the titration rate of Na_2SO_3. The crystallization rate was determined when the amount of calcium sulfite in solution doubled . This rate was then normalized by the BET surface area of the initial seed.

The crystallization rate was correlated as a function of calcium sulfite relative supersaturation. Supersaturations were calculated by the Bechtel-modified Radian Equilibrium Program (12). The relative saturation is defined by:

$$RS_{CaSO_3} = \frac{a_{Ca^{++}} a_{SO_3^{=}}}{K_{sp}} \qquad (10)$$

The value of the K_{sp} used in the correlation was based on the K_{sp} determined in the dissolution experiments.

Results and Discussion: Dissolution

The calcium sulfite hemihydrate dissolution rates were measured for platelet seed crystals with different sulfate contents. The pH was varied from 3.5 to 4.2. The results are compared to previous work by Tseng (8) in which the seed crystals were agglomerates.

Effects of Particle Size/Shape and Sulfate Content in the Solids

The dissolution rate constant is plotted as a function of pH for the two platelet samples in Figure 3. The curves given in Figure 3 were calculated by the stagnant solution mass transfer model. The Sherwood number (Sh) and the solubility product (K_{sp}) were adjusted to give the best fit of the model for each seed crystal and each sulfate solution concentration (Table 1).

The dissolution rate appears to be affected by both particle shape and the sulfate content of the solids. The low sulfate platelets (sample 1) dissolved slower than the other two samples and had the lowest equilibrium pH. The high sulfate platelets (sample 2) dissolved at approximately the same rate as the agglomerated samples, but sample 2 had a

slightly higher equilibrium pH than the agglomerates. This is reflected in the values of the Sherwood number and K_{sp} determined for each seed crystal. The K_{sp} increased as the BET surface area of the solids increased. The Sherwood number reflects the changes in particle size and shape. In these experiments the Sherwood numbers for thin platelets (sample 2) and agglomerates are 3.0 to 3.4. The Sherwood number for non-porous spheres is 2.0. Agglomerates can be thought of as porous spheres. The surface-area-to-volume ratio and effective diameter for the agglomerates are larger than for spheres. Therefore the Sherwood number for agglomerates is larger than for spheres. The thicker platelets (sample 1) have a surface-area-to-volume ratio closer to that of spheres and should have a lower Sherwood number than agglomerates. This is confirmed by a Sherwood number of 2.0 for sample 1.

Effects of Dissolved Sulfate

The effects of sulfate were determined by adding 10 mM Na_2SO_4 to the reactor solution. This corresponds to a gypsum saturation of 1.0 (12). Figure 3 is a plot of the experimental rate constant as a function of pH. The presence of sulfate inhibits the dissolution rate of platelet calcium sulfite at low and high values of pH. Tseng (8) found that sulfate in solution also inhibited the dissolution rate of agglomerated calcium sulfate. The amount that the rate decreased is approximately the same for sample 2 and the agglomerates. Sulfate in solution has a slightly greater inhibiting effect on sample 1 with low sulfate and low surface area.

The mass transfer model can be used to model these results by reducing the Sherwood number and K_{sp} (Table 3). This suggests that dissolution of calcium sulfite in the presence of sulfate is still mass transfer controlled, but the effective area for dissolution is reduced (8).

Results and Discussion: Crystallization

The calcium sulfite crystallization rates were measured for platelet seed crystals with different sulfate contents. The solution pH was varied from 4.7 to 6.0. This corresponds to a calcium sulfite relative saturation of approximately 2 to 15. Sulfate was added to the reactor solution at pH 5.25 to quantify the inhibiting effect of sulfate on platelet calcium sulfite. The results are compared with previous work by Tseng (9) in which the seed crystals were agglomerates.

Crystallization Rate Correlation

The crystallization rate determined by Tseng (9) with agglomerate seed crystals was found to be second order relative to the supersaturation of calcium sulfite and inversely proportional to gypsum saturation (Equation 11).

$$R\left(\frac{\text{mole}}{\text{min-cm}^2}\right) = 9.7\text{x}10^{-4} e^{(-10250/RT)} \frac{(RS_{CaSO_3} - 1)^2}{RS_{CaSO_4}} \qquad (11)$$

The gypsum saturation was taken to be 0.025 when no sulfate was added to the reactor.

Figure 4 is a plot of the crystallization rate as a function of relative supersaturation for the two platelet seed crystals and the agglomerates previously studied by Tseng. The order of calcium sulfite supersaturation dependence is 3.1 and 2.7 for platelet samples 1 and 2, respectively. This is higher than the second order dependence determined by Tseng. Data taken at high calcium sulfite relative saturations were excluded from this analysis. At high saturations the crystallization rate was very fast. Nucleation and crystal growth occurred before the seed crystals could be added to the reactor.

Effect of Gypsum Saturation

The effect of dissolved sulfate on the crystallization rate of platelet calcium sulfite was determined by varying the gypsum saturation from 0.025 to 2.0 at a set pH (5.25). Table 3 is a summary of these results. The crystallization rate decreased as the dissolved sulfate increased.

Tseng (9) found that crystallization rate was inversely proportional to gypsum saturation. Correlation of sample 1 data results in a slightly higher sulfate dependence (Equation 12).

$$\text{Rate} \propto (RS_{CaSO_4})^{-1.5} \qquad (12)$$

Summary

The dissolution and crystallization rates of platelet samples of calcium sulfite were measured at conditions typical of flue gas desulfurization processes. The results were compared with previous work by Tseng (8,9) in which an agglomerated sample was used as the seed crystal.

It was determined that there are subtle differences between platelet and agglomerated calcium sulfite. The platelet sample with the low solid sulfate content (sample 1) dissolved and crystallized slower than the other samples. The inhibiting effect of dissolved sulfate was also greater for sample 1. The sample with a high solid sulfate content (sample 2) dissolved and crystallized at approximately the same rate as the agglomerates.

Acknowledgement

This work was supported by EPA Cooperative Agreement CR812454.

Nomenclature

a	activity (M)
C	solute concentration in bulk liquid (M)
C_s	solute concentration at particle surface (M)
d_p	particle diameter (cm)
D	Ca^{++} diffusivity (cm^2/sec)
F	total fraction of particles remaining
k	dissolution rate constant (cm^2/sec)
k_c	mass transfer coefficient (cm/sec)
K_a	equilibrium constant
K_{sp}	calcium sulfite solubility product (M^2)
M	molarity (mole/liter)
R	crystallization rate based on BET surface area (mole/min-cm^2)
RS	relative saturation
Sh	Sherwood number
t	time (sec)
T	temperature (K)
V	volume of single particle (cm^3)
V_T	total volume of particles (cm^3)
V_0	total inital volume of particles (cm^3)

Greek Symbols

ρ	crystal density (0.0194 mole/cm^3)
ϕ_j	fraction of total particle volume with diameters from d_j to d_{j+1}

TABLE 1. Characteristics of Seed Crystals, Adjusted Sherwood Number, and K_{sp} of Calcium Sulfite
(0.1 M $CaCl_2$, 10 mM Na_2SO_3, 23°C)

Crystal Habit (8,9)	Platelets		Agglomerates		
Sample No.	1	2	Seed 1	Seed 3	Seed 5
$CaSO_4$ Content (mole %)	2.4	15	3.4	10.7	1.0
BET Surface Area (m^2/g)	1.0	2.8	1.9	9.5	1.2
Median Size (μm)	16	14	16	13	18
$K_{sp} \times 10^7$(no sulfate) (M^2)	2.65	3.80	3.46 *	3.91 *	3.29 *
Sh (no sulfate)	2.0	3.8	3.4	3.8	4.0
$K_{sp} \times 10^7$(10 mM sulfate)(M^2)	2.16	3.42	-	-	-
Sh (10mM sulfate)	0.3	1.4	-	-	-

* Corrected value of K_{sp}; value reported incorrectly in References 8 and 9.

TABLE 2. Calcium Sulfite Particle Size Distributions

Effective Diameter-upper limit (μm)	$CaSO_3$ Volume Percent	
	Sample Number 1	2
2.0		0.1
3.17		0.6
4.00		1.0
5.04	1.8	2.3
6.35	2.8	3.9
8.00	4.7	5.4
10.08	7.5	9.5
12.7	11.9	12.2
16.0	15.2	14.1
20.2	16.4	14.9
25.4	15.0	11.7
32.0	11.3	9.7
40.3	6.9	5.6
50.8	3.4	3.8
64.0	2.0	1.7
80.6	0.9	1.5
101.6	0.2	0.7
128.0		0.8
161.0		0.3

TABLE 3. Effects of Gypsum Saturation on the Crystallization Rate of Calcium Sulfite Seed Crystals
(0.1 M $CaCl_2$, 10 mM Na_2SO_3, pH 5.25, 23°C)

Seed Crystal	RS_{CaSO_4}	Rate (moles/min-cm^2)
Sample 1	0.025	2.94×10^{-8}
	0.5	8.9×10^{-9}
	1.0	6.4×10^{-9}
	2.0	1.1×10^{-9}
Sample 2	0.025	4.0×10^{-8}
	0.5	4.0×10^{-9}
Agglomerates (9,10) Seed 1	0.025	2.0×10^{-8}
	1.9	6.1×10^{-10}

Reproduced from
best available copy.

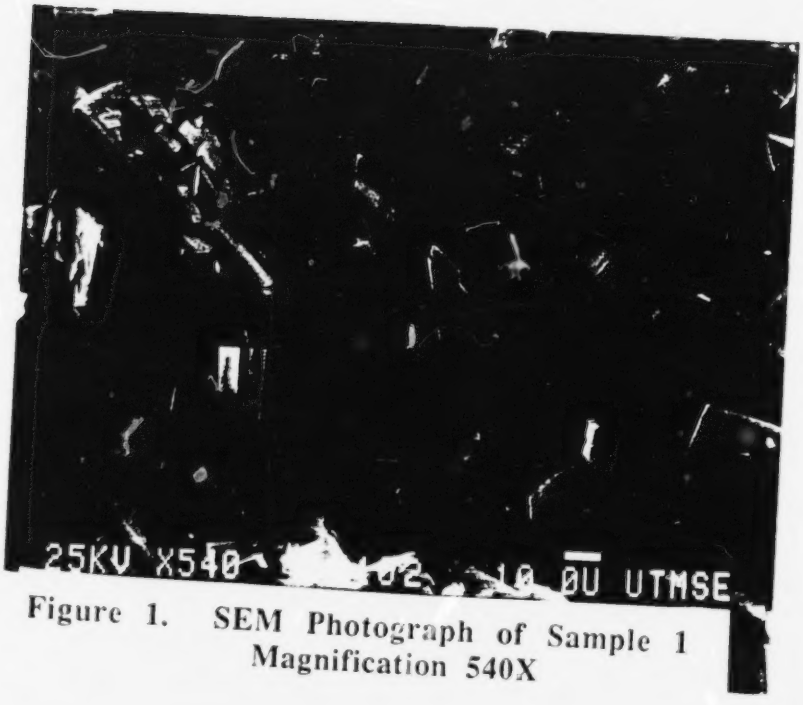

Figure 1. SEM Photograph of Sample 1
Magnification 540X

Figure 2. SEM Photograph of Sample 2
Magnification 600X

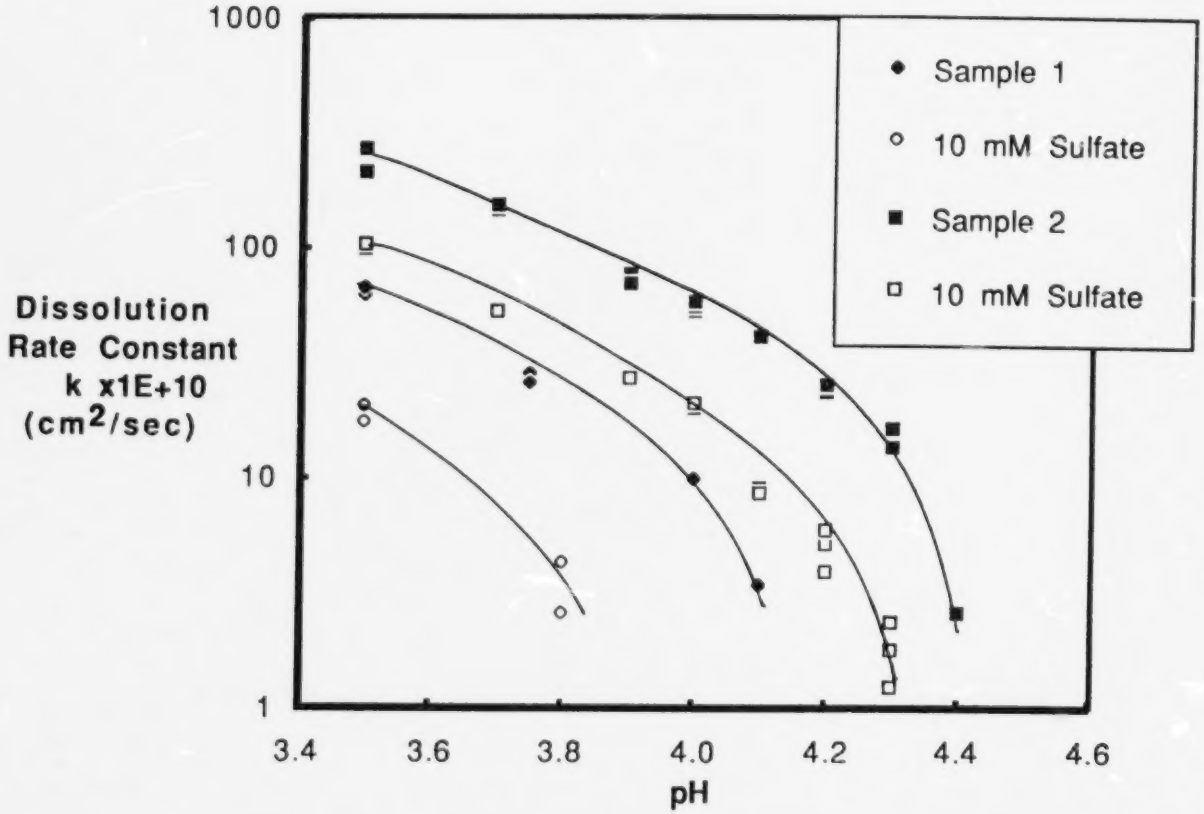

Figure 3. Effects of Solid and Dissolved Sulfate Content on Calcium Sulfite Dissolution Rates and Equilibrium pH.
(0.1 M $CaCl_2$, 10 mM Na_2SO_3, 23°C;
Curves calculated by the mass transfer model)

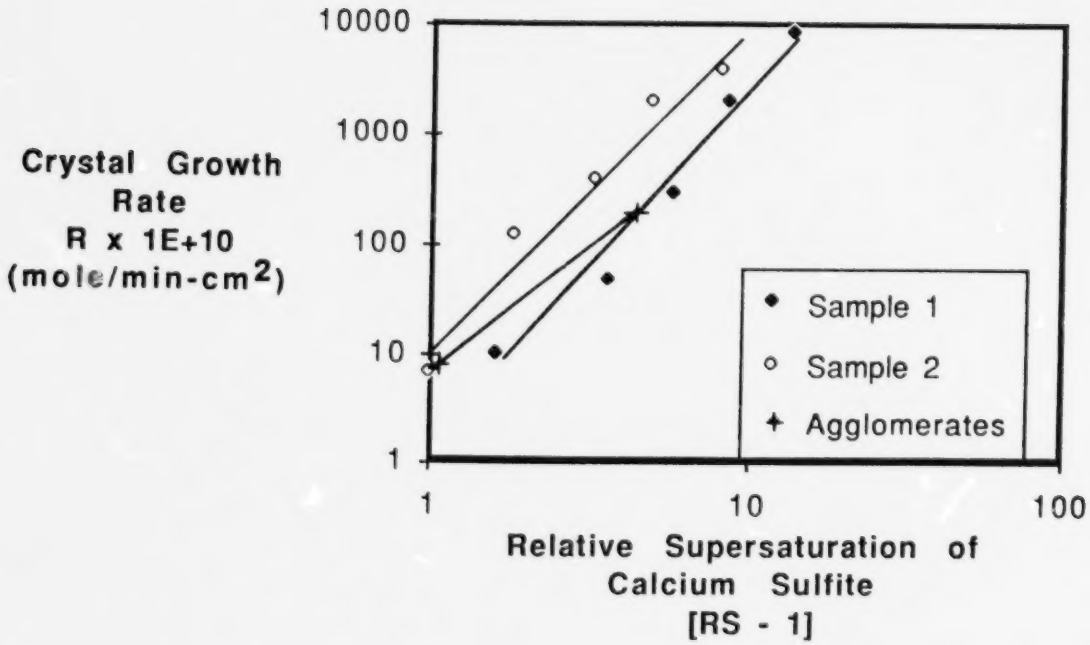

Figure 4. Calcium Sulfite Crystallization Rate
(0.1 M $CaCl_2$, 10 mM Na_2SO_3, 23°C)

References

1. Chan, P.K. and G. T. Rochelle, "Limestone Dissolution: Effects of pH, CO_2 and Buffers Modeled by Mass Transfer", ACS Symp. Ser., 188, 75-97 (1982).

2. Ottmers, D., J. Phillips, C. Burklin, W. Corbett, N. Phillips, and C. Shelton, "A Theoretical and Experimental Study of the Lime/Limestone Wet Scrubbing Process", EPA-650/2-75-006 (PB 243-399/AS), December (1974).

3. Jones, B. J., P. S. Lowell, and F. B. Meserole, "Experimental and Theoretical Studies of Solid Solution Formation in Lime and Limestone SO_2 Scrubbers", EPA-600/2-76-273a (PB 264-953/AS),Vol I,October (1976).

4. Setoyama, K. and S. Takahashi, "Solid Solution of Calcium Sulfite Hemihydrate and Calcium Sulfate", Yogyo-Kyokai-Shi, 86, 56-62 (1978).

5. Edwards, L. O., "Calcium Sulfite Crystal Sizing Studies", EPA-600/7-79-192 (PB 80-128-689), August (1979).

6. Kelly, B. J., "Study of Calcium Sulfite Hemihydrate Nucleation and Growth Rates in Simulated Flue-Gas Desulfurization Liquors", MS Thesis, University of Arizona (1983).

7. Alvarez-Dalama, A., "Calcium Sulfite Hemihydrate Crystallization in Liquors with High Total Dissolved Solids", MS Thesis, University of Arizona (1986).

8. Tseng, P.C. and G.T. Rochelle, "Dissolution Rate of Calcium Sulfite Hemihydrate in Flue Gas Desulfurization Processes", Env. Prog., 5, 35-40 (1986).

9. Tseng, P.C. and G.T, Rochelle,"Calcium Sulfite Hemihydrate: Crystal Growth Rate and Crystal Habit", Env. Prog., 5, 5-11 (1986).

10. Tseng, P. C., "Calcium Sulfite Hemihydrate Dissolution and Crystallization", PhD Dissertation, University of Texas Austin (1983).

11. Toprac, A. J., "Limestone Dissolution in Stack Gas Desulfurization", Environ. Prog., 1, 52-58(1982).

12. Lowell, P.S., D.M. Ottmers, K. Schwitzgebel, T.I. Strange, and D.W. Deberry , "A Theoretical Description of the Limestone Injection Wet Scrubbing Process", EPA Report APTD 1287 (PB 193-029), Vol I, June(1970).